

Effects of Mass Transfer on Unsteady Free Convection MHD Flow Between Two Heated Vertical Plates in the Presence of Transverse Magnetic Field

BHASKAR KALITA

Associate Professor, Department- Mathematics

T. H. B. College, Jamugurihat, Sonitpur, Assam

e-mail - drbhaskarkalita@yahoo.com

Abstract: In this work a study is presented of the effects of mass transfer on unsteady free convection flow of an incompressible viscous fluid past between two heated vertical parallel plates under uniform transverse magnetic field. An analytical solution for the problem under consideration has been obtained using the Laplace Transform Method [7]. The effects of the concentration parameter Sc (Schmidt number), the magnetic parameter M , the viscosity-heat conduction parameter Pr (Prandtl number) together with variation of time, have been examined on the flow of fluid velocity, temperature and concentration. The analytical results have shown that the above mentioned effects have to be taken into consideration in the flow of fluid, heat and mass transfer processes.

Keywords: Unsteady free convection MHD flow, Mass transfer, Laplace Transformation

Subject Classification: 76W05

1. Introduction:

It has been seen by long experience that, in many engineering activities, especially in chemical engineering, that some processes are considered to be the mass transfer processes, which are sometimes accompanied by many other processes like heat transfer, rotation of fluids, electromagnetic forces, etc. The random movement of the molecules, which by their mixing tend to equalize existing differences in their energy, causes the heat conduction in a gas. By the same movement local differences in concentration of a gas mixture diminished in time even if no macroscopic mixing occurs. This process is known as diffusion. By diffusion or convection, in a mixture of local concentration differences, a component is transported from one location to another. The mass transport through an interface between various phases of the same medium is found to be a special important in engineering sciences.

The range of free-convection flows that occur in nature and in engineering practices is vast and significant. So far, many papers, both theoretical and experimental, have been published on free convection heat transfer in view of their interest in astrophysics, geophysics, engineering and medical sciences. However, the flow of a fluid is caused not only by the temperature differences but also by concentration differences. These concentration differences also affect the flow and temperature near the surface of a body embedded in a fluid. In engineering applications, the

We consider a vertical channel bounded by two fixed vertical parallel infinite plates and both are at the same temperature T'_0 , initially. At time $t' > 0$, the plates are supplied heat at constant rate, thereby causing the presence of free convection currents in the fluid near the plates. As the plates are infinite in extent, the flow-variables are functions of y' and t' . The x' – axis is taken along the plates in the vertically upward direction and the y' – axis is taken normal to the plates. The uniform magnetic field B_0 is applied along horizontal direction, i.e. in a direction perpendicular to the fluid motion.

Under the above assumptions following Boussinesq's approximation, the flow fields are seem to be governed by the following equations:

Equation of mass conservation:

$$\frac{\partial v'}{\partial y'} = 0 \quad (1)$$

Equation of momentum:

$$\frac{\partial u'}{\partial t'} = \frac{\mu}{\rho} \frac{\partial}{\partial y'} \left(\mu \frac{\partial u'}{\partial y'} \right) + g\beta(T' - T_0) + g\beta^*(C' - C_0) - \frac{\sigma}{\rho} B^2 u' \quad (2)$$

Equation of energy:

$$\rho C_p \frac{\partial T'}{\partial t'} = K \frac{\partial^2 T'}{\partial y'^2} \quad (3)$$

Equation of diffusion:

$$\frac{\partial C'}{\partial t'} = D \frac{\partial^2 C'}{\partial y'^2} \quad (4)$$

At time $t' > 0$, the temperature of the plates ($y = \pm h$) changes according to $T' = T'_0 + (T'_w - T'_0)(1 - e^{-n't'})$, where n' is a decay factor,

The concentration of the fluid changes according as $C' = C'_0 + (C'_w - C'_0)(1 - e^{-n't'})$.

At any time t' , the velocity, the temperature and the concentration are given by (u', o, o) , T' and C' , respectively.

The initial and boundary conditions are given by-

$$\begin{aligned} u' = 0, \quad T' = T'_0, \quad C' = C'_0 & \quad \text{for all } y \in [-h, h], t' = 0 \\ u' = 0, \quad T' = T'_0 + (T'_w - T'_0)(1 - e^{-n't'}) & \quad \text{for } y = \pm h \\ C' = C'_0 + (C'_w - C'_0)(1 - e^{-n't'}) & \quad \text{for } y = \pm h \end{aligned} \quad (5)$$

The dimensionless quantities which we used are-

$$u = \frac{u'h}{\nu}, T = \frac{T' - T'_0}{T'_w - T'_0}, C = \frac{C' - C'_0}{C'_w - C'_0}, t = \frac{t'\nu}{h^2}, y = \frac{y'}{h}, n = \frac{n'h^2}{\nu}$$

$$\text{Pr} = \frac{\rho\nu C_p}{K} \quad \text{Gr}_t = \frac{g\beta h^3 (T'_w - T'_0)}{\nu^2} \quad \text{Gr}_m = \frac{g\beta^* h^3 (C'_w - C'_0)}{\nu^2}$$

$$M = B_0 h \sqrt{\frac{\sigma}{\mu}} \quad Sc = \frac{\nu}{D} \quad (6)$$

Using the dimensionless quantities (2-6), the equations (2-2) - (2-4) together with the boundary conditions (2-5), are found as follows:

$$\frac{\partial u}{\partial t} = \frac{\partial^2 u}{\partial y^2} + Gr_i T + Gr_m C - M^2 u \quad (7)$$

$$\frac{\partial T}{\partial t} = \frac{1}{Pr} \frac{\partial^2 T}{\partial y^2} \quad (8)$$

$$\frac{\partial C}{\partial t} = \frac{1}{Sc} \frac{\partial^2 C}{\partial y^2} \quad (9)$$

$$\begin{aligned} u = 0, \quad T = 0, \quad C = 0 \quad \text{for all } y \in [-1, +1], \quad t = 0 \\ u = 0, \quad T = 1 - e^{-nt}, \quad C = 1 - e^{-nt} \quad \text{for } y = \pm 1 \end{aligned} \quad (10)$$

3. Solution of the equations:

Taking the Laplace Transform of equations (2-7) - (2-10), we get

$$\frac{d^2 \bar{u}}{dy^2} - (M^2 + s) \bar{u} = -(Gr_i \bar{T} + Gr_m \bar{C}) \quad (11)$$

$$\frac{d^2 \bar{T}}{dy^2} - Pr.s.\bar{T} = 0 \quad (12)$$

$$\frac{d^2 \bar{C}}{dy^2} - Sc.s.\bar{C} = 0 \quad (13)$$

where

$$\bar{F}(y, s) = \int_0^{\infty} e^{-st} F(y, t) dt$$

together with boundary conditions

$$\bar{u}(\pm 1, s) = 0, \quad \bar{T}(\pm 1, s) = \frac{n}{s(s+n)}, \quad \bar{C}(\pm 1, s) = \frac{n}{s(s+n)} \quad (14)$$

Since, the equations (2-11) – (2-13) are of 2nd order ordinary differential equations in \bar{u}, \bar{T} and \bar{C} , the solutions of the equations by use of boundary conditions (2-14), are found as -

$$\bar{T} = \frac{n}{s(s+n)} \cdot \frac{\cosh \sqrt{s Pr} \cdot y}{\cosh \sqrt{Pr} \cdot s} \quad (15)$$

$$\bar{C} = \frac{n}{s(s+n)} \cdot \frac{\cosh \sqrt{s.Sc} y}{\cosh \sqrt{s.Sc}} \quad (16)$$

$$\begin{aligned} \bar{u} = & -\frac{n}{s(s+n)} \left[\frac{Gr_t}{s(1-Pr)+M^2} + \frac{Gr_m}{s(1-Sc)+M^2} \right] \frac{\cosh \sqrt{M^2+s} y}{\cosh \sqrt{M^2+s}} \\ & + \frac{n}{s(s+n)} \left[\frac{Gr_t}{s(1-Pr)+M^2} \frac{\cosh \sqrt{s.Pr} y}{\cosh \sqrt{s.Pr}} + \frac{Gr_m}{s(1-Sc)+M^2} \cdot \frac{\cosh \sqrt{Sc.s} y}{\cosh \sqrt{Sc.s}} \right] \end{aligned} \quad (17)$$

The inverse Laplace Transform of (15) – (17), gives the actual solution as –

$$T = 1 - \frac{\cos \sqrt{n.Pr} y \cdot e^{-nt}}{\cos \sqrt{n.Pr}} + \frac{4n}{\pi} \sum_{k=0}^{\infty} \frac{(-1)^k \cos \frac{(2k+1)\pi y}{2} e^{-\frac{(2k+1)^2 \pi^2}{4.Pr} t}}{(2k+1) \left\{ \frac{(2k+1)^2 \pi^2}{4.Pr} - n \right\}} \quad (18)$$

$$C = 1 - \frac{\cos \sqrt{n.Sc} y \exp(-nt)}{\cos \sqrt{n.Sc}} + \frac{4n}{\pi} \sum_{k=0}^{\infty} \frac{(-1)^k \cos \frac{(2k+1)\pi y}{2} \cdot \exp(-(2k+1)^2 \pi^2 t / 4.Sc)}{(2k+1) \left\{ \frac{(2k+1)^2 \pi^2}{4.Sc} - n \right\}} \quad (19)$$

$$\begin{aligned} u = & \frac{Gr_t + Gr_m}{M^2} \left[1 - \frac{\cosh My}{\cosh M} \right] - \frac{Gr_t \exp(-nt)}{n(1-Pr) - M^2} \left[\frac{\cos \sqrt{n-M^2} y}{\cos \sqrt{n-M^2}} - \frac{\cos \sqrt{n.Pr} y}{\cos \sqrt{n.Pr}} \right] \\ & - \frac{Gr_m \exp(-nt)}{n(1-Sc) - M^2} \left[\frac{\cos \sqrt{n-M^2} y}{\cos \sqrt{n-M^2}} - \frac{\cos \sqrt{n.Sc} y}{\cos \sqrt{n.Sc}} \right] + 4n\pi \times \\ & \sum_{k=0}^{\infty} \frac{(-1)^k (2k+1) \cos((2k+1)\pi y / 2) \exp(-(M^2 + (2k+1)^2 \pi^2 / 4)t)}{\{M^2 + ((2k+1)^2 \pi^2 / 4)\} \{M^2 + ((2k+1)^2 \pi^2 / 4) - n\}} \times \\ & \left[\frac{Gr_t}{(1-Pr) - \{M^2 / (M^2 + (2k+1)^2 \pi^2 / 4)\}} + \frac{Gr_m}{(1-Sc) - \{M^2 / (M^2 + (2k+1)^2 \pi^2 / 4)\}} \right] \\ & + \frac{4n}{\pi} \sum_{k=0}^{\infty} \frac{(-1)^k \cos((2k+1)\pi y / 2)}{2k+1} \times \left[\frac{Gr_t \exp(-(2k+1)^2 \pi^2 t / 4.Pr)}{\{(2k+1)^2 \pi^2 / 4.Pr - n\} \{M^2 - (1-Pr)(2k+1)^2 \pi^2 / 4.Pr\}} + \right. \\ & \left. \frac{Gr_m \exp(-(2k+1)^2 \pi^2 t / 4.Sc)}{\{(2k+1)^2 \pi^2 / 4.Sc - n\} \{M^2 - (1-Sc)(2k+1)^2 \pi^2 / 4.Sc\}} \right] \end{aligned} \quad (20)$$

4. Results and Discussion:

In this section, we summarize the most important findings uncovered in this investigation and present the supporting results through graphs and tabular values. All figures and tables appearing in this work were generated directly from the exact solution / expressions given in § 3 using scientific calculator first, and later on by C – program. Both the obtained results and data are same upto 10th decimal places in all cases. To simplify our discussion, we choose the decay factor n and Magnetic Hartmann number M in such a way that there does not appear negative number under the square roots. Hence, based on certain and standard values of different parameters and numbers, we state the following.

Figure 1 has been obtained by plotting the temperature distribution T against y at different times when $n = 1$, $Pr = .025$. This figure shows that the temperature at any point increases with the increase of t . It is seen that the difference of distribution of temperature in between $t = 1$ and $t = 2$ is large while in between $t = 2$ and $t = 3$ is small. It seems that there will be no increase of temperature distribution though time would be increased.

The temperature profiles have been drawn for $t = .1$, $Pr = .025$, and for different values of temperature decay factor n , in figure 2. It is found from this figure that the temperature at any point inside the vertical channel increases with the increase of n , and it flows with higher values at and near the walls than at the middle of the channel. This values of T uniformly decreases from the wall and minimum value occurs at $y = 0$.

Figure 3 has been drawn to show the effect of Prandtl number (Pr) on temperature distribution. This investigation shows that for any value of Pr , at the closed region of the walls, the values of the temperature distribution is the same; but at the middle of the channel it varies significantly. Towards the middle of the channel, the temperature distribution decreases as Prandtl number increases.

In figure 4, we have investigated the mass diffusion (C) against y inside the channel in the presence of temperature decay factor $n (=1)$ and Schmidt number $Sc (= .22)$ with respect to small time ($t = .1$) and large time ($t = 1, 2, 3$). A clear difference of mass diffusion for small and large time had been noticed. The difference is about to end after time $t = 3$, also diffusion rate is slow at the middle of the channel.

The figure 5, has been drawn to show the effect of temperature factor (n) on mass diffusion at time $t = .5$ and Schmidt number $Sc = .22$. The graph obtained for $n = 5$, shows that the diffusion difference is very high, highest near the walls. This means that at the center of the channel the diffusion rate is very slow. Most intriguingly, however, for $n = 15$, the diffusion processes is same at all regions of the channel. Perhaps the mass diffusing processes come to an end for values of n greater than 15.

The figure 6 has been drawn to show how various species diffuses at same time ($t = .5$, here), and temperature factor ($n = 1$, here). It has been observed that as the values of the Schmidt number, Sc , increases the diffusion difference increases. For $Sc = 0$, the rate of mass diffusion is similar in all regions of the channel.

We have considered the figure 7 to show the effect on velocity profiles caused at different times with respect to standard fixed values of the parameters considered. From the figure, it is observed that for smaller times the flow distribution differs greatly than the larger times inside the channel; even for $t = 2$ and $t = 3$, the differences in values of u are very negligible. Moreover, the difference appears only after 3 digits of decimal place, which as a result ca' not be seen any difference in the figure.

In figure 8, we have shown the effect of magnetic field parameter M on velocity profiles for standard fixed values of different parameters as shown in figure. It is seen that as M increases u decreases. However, this is interesting to note that the flow field neither depends solely on M but also on n. This can be seen in analytical result in §3, under radical sign and on graphical vision in the figure.

Figure 9 has been drawn to show the effect of temperature factor (n) on velocity profiles at small time as well as at large time for fixed values of different parameters that appears under assumption. It is clearly observed that for $t = .1$ and $n = 5$, the flow distribution differs greatly than for $t = 1$ and $n = 5$. From this we confer that as time advances the flow distribution difference decreases. Again we see the effect of temperature decay factor n on velocity field. As the values of n increases, the corresponding values of u first increases, later on decreases; even at the middle of the channel. It is also the sign of stream -lines flow situation.

The velocity profiles have been plotted against y for $n = 1$, $Pr = .025$, $Sc = .22$, $M = .5$ and for various values of Grashof number (Gr_m) in figure 10. The profiles are studied at two different times. It is seen that as the values of Gr_m increases the values of velocity field also increases at time $t = .5$; but at time $t = 2$ and for $Gr_m = 4$, it seems to decrease. Thereby it means that the flow field seems to attain the fully developed situation after time $t = 2$. The calculation done for small time shows that the increase of concentration also increases the difference of diffusion.

The view taken in figure 11 is one looking down upon the two different values of Prandtl number (Pr) at two different time. The plotted graphs clearly show that as Pr increases in turn the velocity field decreases. If we look down upon the time factor, it clearly suggests the idea that as time increases, the difference of flow distribution decreases irrespective of the kinds of electrically conducting fluid. It gives hints of matured mixture and fully developed situation at large time.

Figure 12 illustrates the temporal evaluation of the flow pattern caused by varying values of Prandtl number (Pr) and magnetic Hartman number (M), simultaneously at fixed values of other parameters and time. It is seen that as Pr and M increases simultaneously, the values of u decreases at the center of the channel. However, any change of Prandtl and Hartmann number do not affect on the velocity distribution near the two walls.

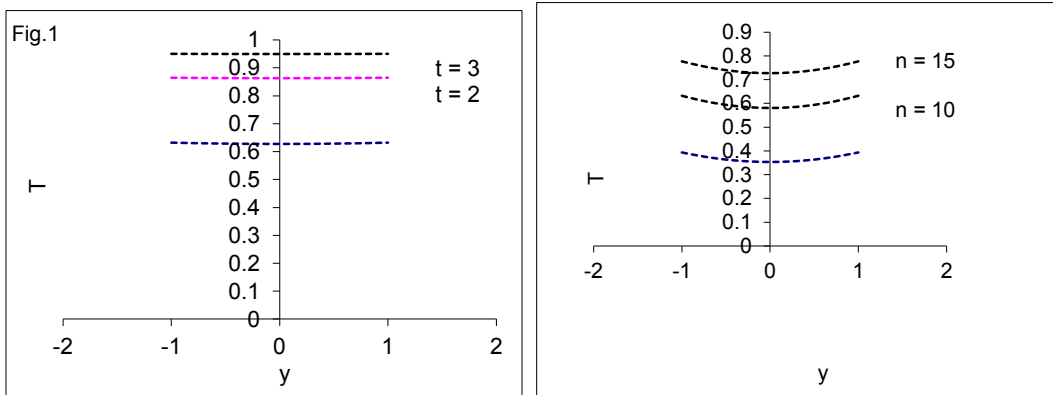


Fig. 1: T versus y for $Pr = .025$, $n = 1$ at time $t = 1, 2, 3$ Fig. 2: T versus y for $Pr = .025$, $t = .1$, at $n = 5, 10, 15$

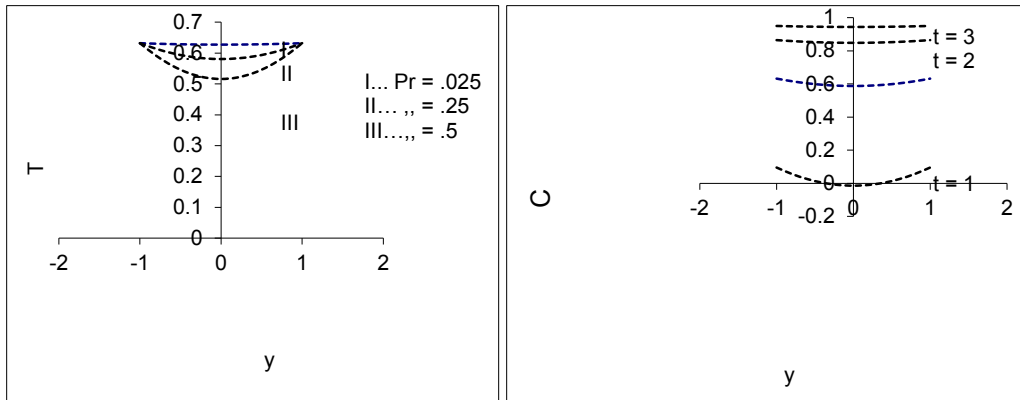


Fig.-3: T versus y for $Pr = .025, .25, .5$ at $t = 1, n = 1$ Fig. -4: C versus y for $n = 1, Sc = .22$ at $t = .1, 1, 2, 3$

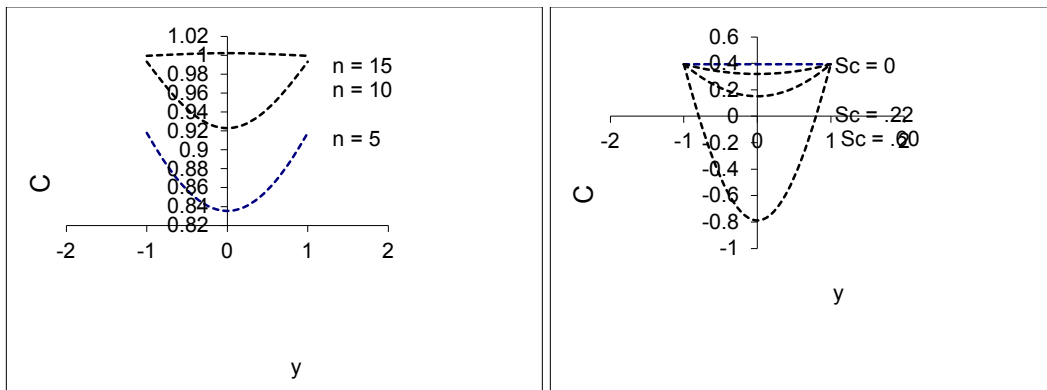


Fig. -5: C versus y for $t = .5, Sc = .22, n = 5, 10, 15$ Fig.-6: C versus y for $t = .5, n = 1$ at different values of Sc

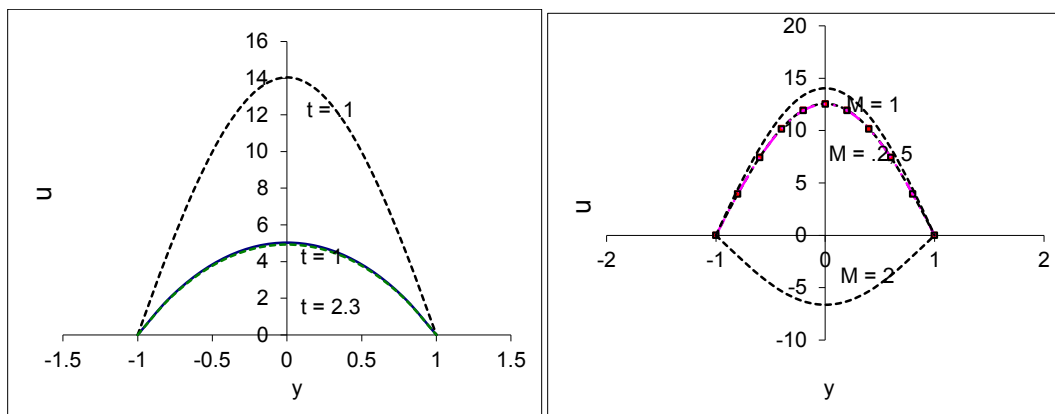


Fig.-7: u versus y for $n = 5, M = 1, Sc = .22$, Fig.-8: u versus for $n = .5, t = .1, Pr = .025, Sc = .22,$
 $Pr = .025, Gr_t = 10, Gr_m = 4$ $Gr_t = 10, Gr_m = 4$

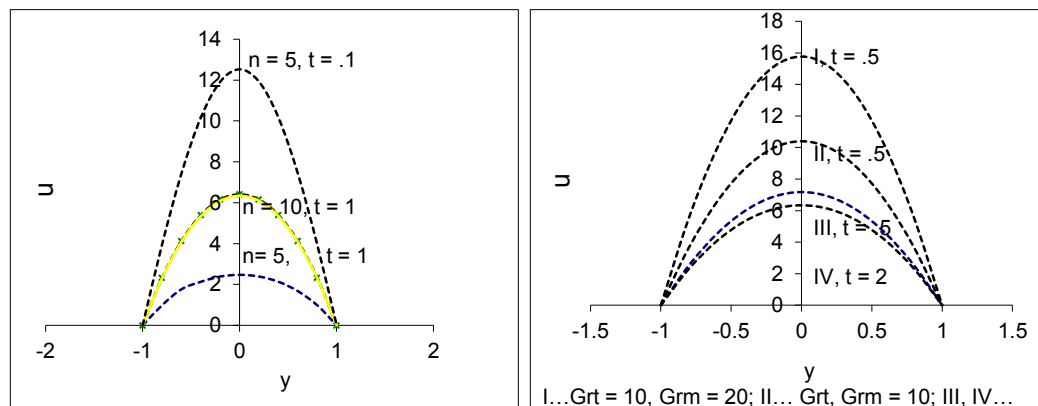


Fig.-9: u versus y for $Pr = .025, M = .5, Sc = .22$, Fig.-10: u versus y for $n = 1, Pr = .025, Sc = .22, M = .5$
 $Gr_t = 10, Gr_m = 4$

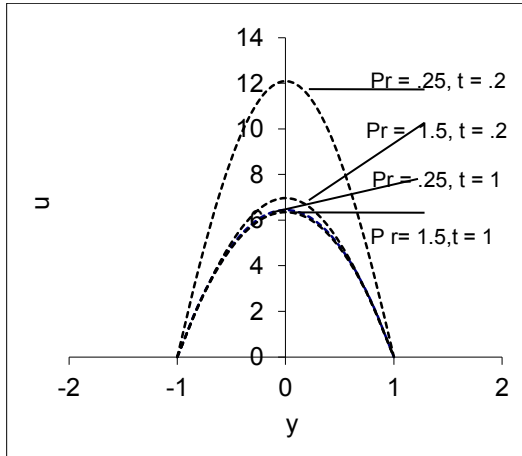


Fig.-11: u versus y for n=5, M=.5, Sc=.22
 $Gr_t = 10, Gr_m = 4$

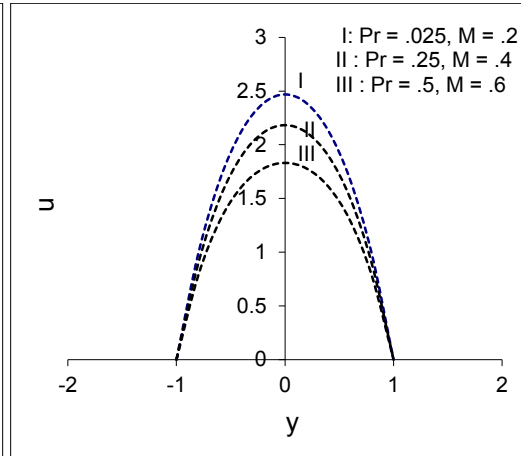


Fig.-12: u versus y for n=1, t=1, Sc=.22,
 $Gr_t = 10, Gr_m = 4$

§ Skin Friction (C_f):

For engineering purposes, one is usually less interested in the shape of the velocity, temperature or concentration profiles than on the values of Skin friction, Heat transfer or Mass transfer parameter. All the values of these letter ones are conventionally described by appropriate coefficients. The following relations define them

$$C_f = \frac{2\tau_w}{\rho U_0^2}, Nu_x = \frac{xq_w}{k(T_w - T_0)}, Nm_x = \frac{h_m x}{D_m(C_w - C_0)} \quad (21)$$

$$\text{where } \tau_w = \left[\mu \frac{\partial u'}{\partial y'} \right]_{y'=\pm h}, q_w = -k \left[\frac{\partial T'}{\partial y'} \right]_{y'=\pm h}, h_m = -D_m \left[\frac{\partial C'}{\partial y'} \right]_{y'=\pm h} \quad (22)$$

But, we have only the skin friction here, as Nu_x (the local Nusselt number) and Nm_x (the local Sherwood number) become zero for T and C being the function of t instead of being function of y. Using (2-6), (2-20) and (2-22), we have (2-21) as

$$C_f = \frac{-2}{Re^2} \left[\frac{Gr_t + Gr_m}{M} \tanh(M) + \frac{Gr_t e^{-nt}}{n(1 - Pr) - M^2} (\sqrt{nPr} \tan \sqrt{nPr} - \sqrt{n - M^2} \tan \sqrt{n - M^2}) \right. \\ \left. + \frac{Gr_m e^{-nt}}{n(1 - Sc) - M^2} (\sqrt{nSc} \tan \sqrt{nSc} - \sqrt{n - M^2} \tan \sqrt{n - M^2}) \right]$$

$$\begin{aligned}
& + \sum_{k=0}^{\infty} \frac{8n(2k+1)^2 \pi^2 e^{-\frac{1}{4}\{4M^2+(2k+1)^2\pi^2\}t}}{\{4M^2+(2k+1)^2\pi^2\} \left\{ \frac{4M^2+(2k+1)^2\pi^2}{4} - n \right\}} \left\{ \frac{Gr_t}{(1-\text{Pr}) - \frac{4M^2}{4M^2+(2k+1)^2\pi^2}} \right. \\
& + \left. \frac{Gr_m}{(1-\text{Sc}) - \frac{4M^2}{4M^2+(2k+1)^2\pi^2}} \right\} + \sum_{k=0}^{\infty} \frac{nGr_t e^{-\frac{(2k+1)^2\pi^2}{4\text{Pr}}t}}{\left(\frac{(2k+1)^2\pi^2}{4\text{Pr}} - n \right) \left(M^2 - (1-\text{Pr}) \frac{(2k+1)^2\pi^2}{4\text{Pr}} \right)} \\
& + 2 \sum_{k=0}^{\infty} \frac{nGr_m e^{-\frac{(2k+1)^2\pi^2}{4\text{Sc}}t}}{\left(\frac{(2k+1)^2\pi^2}{4\text{Sc}} - n \right) \left(M^2 - (1-\text{Sc}) \frac{(2k+1)^2\pi^2}{4\text{Sc}} \right)} \left. \right] \text{Re} = \frac{hU_0}{\nu} \quad (23)
\end{aligned}$$

We have obtained the result of skin friction for the plate at $h = +1$. All the results that would be found for $h = -1$ would have been seemed to be opposite to the results found in tables (1) – (5). Here we have observed the effects of the following dimensionless parameters and decay factor.

- (a) *The effect of Re:* From the table 1, it is seen that the effects of the Reynolds number Re , the dimensionless parameter of the ratio of the inertial motion to the viscous resistance, is prominent in the skin friction. For $Re = 1$, skin friction is the highest, and then it decreases as Reynolds number increases. Other parameters are assumed fixed.
- (b) *The effect of n:* Table 2 has been obtained for various values of n , the temperature decay factor, starting from 1 to 25. It is seen that n plays an important role in the increase or decrease of skin friction. It is difficult to predict the situation that for increasing values of n there would be any increase or decrease in skin friction. This situation particularly depends on magnetic parameter M .
- (c) *The effect on M:* In the table 3 the effect of M on the skin friction has been shown. It is seen that as M increases from .025 to .5, skin friction decreases. However, for other greater values this kind of prediction cannot be done; even we will face domain error if we would consider the values, which are greater than square root values of n .
- The effects of Pr and Sc:* We have deduced the values of skin friction for different values of Pr and Sc at two values of Re and fixed values of other parameters in table 4. It is obvious from the table that for Reynolds number = 1300 skin friction is negligible, while for $Re = 1$, it is significant. Moreover, for different pair values of Pr and Sc , we see different skin friction. For higher values of
- (d) these two, C_f is negative. Alternately, for smaller and standard values, it is positive and remarkable.
- (e) *The effects of Gr_t and Gr_m :* Lastly, in table 5, we have given the variation in Gr_t and Gr_m to show its effect on skin friction. For high Reynolds number, the effects of these parameters are not significant, but for small Reynolds numbers these parameters are countable.

Table 1. Values of C_f for different values of Reynolds number (Re) when			
$n = 5, t = .1, Gr_t = 10, Gr_m = 20, Pr = .025, Sc = .22, M = .5$			
<u>Re</u>	<u>C_f</u>	<u>Re</u>	<u>C_f</u>
1	758.79895	10	7.588047
100	0.075880	200	0.01897
500	0.003035	1000	0.000759
1200	0.000527	1300	0.000449
1500	0.000337	2000	0.00019
2200	0.000157	2500	0.000121

Table 2. Values of C_f for different values of decay factor (n) at			
$Gr_t = 10, Gr_m = 20, M = .5, Re = 10, Sc = .22, t = 1, Pr = .025$			
<u>n</u>	<u>C_f</u>	<u>n</u>	<u>C_f</u>
1	- 0.437598	2	- 1.237877
3	2.843106	4	0.498329
5	0.195368	7	0.008061
10	- 0.081594	15	- 0.133889
20	- 0.155934	25	- 0.168086

Table 3. Variation of skin friction C_f for different values of M at			
$Gr_t = 10, Gr_m = 20, Pr = .025, Sc = .22, t = 1, n = 5, Re = 1300$			
<u>M</u>	<u>C_f</u>	<u>M</u>	<u>C_f</u>
.025	0.357097	.1	0.349901
.25	0.311365	.5	0.195368
1.0	- 0.048251	1.5	0.069489
2.0	- 0.291442	2.2	- 0.262698

Table 4. Skin friction C_f for various values of Pr and Sc when			
$Gr_t = 10, Gr_m = 20, M = .5, n = 5, t = 1, Re = 1, 1300$			
<u>Pr</u>	<u>Sc</u>	<u>C_f (Re = 1)</u>	<u>C_f (Re = 1300)</u>
0.025	0.22	19.536825	0.000012
0.25	0.60	73.327301	0.000043
0.50	0.60	86.569122	0.000051
0.71	0.22	65.498520	0.000039
0.71	1.00	- 2722013.5	- 1.610659
1.00	1.00	- 4083093.5	- 3.756418
2.00	1.50	- 128.387253	- .000076

Table 5. Variation of skin friction C_f for different values of Gr_t and Gr_m at
 $Pr = .025, t = 1, M = .5, n = 5, Sc = .22$

Gr_t	Gr_m	C_f (Re=10)	C_f (Re=1300)
2.0	2.0	0.022515	0.000001
2.0	4.0	0.039074	0.000002
10	4.0	0.062896	0.000004
20	10	0.142352	0.000008
10	20	0.195368	0.000012
10	100	0.857728	0.000051

References

1. Kalita, B. and Borkakoti, A. K.: Unsteady flow and heat transfer between two horizontal plate in the presence of magnetic field (one plate adiabatic). 2006. Ph. D. Thesis. Tezpur University, India.
2. Soundalgekar, V. M., Deka, R. K. and Das, U. N. Transient free convection flow of a viscous incompressible fluid past an infinite vertical plate with periodic heat flux, Indian J. Engg. Materials Sci. 10, 390-396, (2003).
3. Jordan, P. M. and Puri, P. Exact solutions of the unsteady plane couette flow of a dipolar fluid. Proc. Of Royal Soci. of London, 1245-1272 (2002).
4. Gourela, M. G. & Katoch, S., Unsteady free convection MHD flow between heated vertical plates, Ganita, Vol. 42, No. 2, 143 – 154, (1991).
5. Kafoussias, N. G.: Effect of mass transfer on free convective flow past a vertical isothermal cone surface, "Int. J. Engineering Sciences", Vol. 30, No. 273 – 281, 1992
6. Sherclif, J. A. " A text book of Magnetohydrodynamics", Pergamon Press, 1965
7. Spiegel, R. Murray, "Laplace Transform", Schaum's Outline Series, McGRAW- Hill Book Company, 1986.
8. Das, U. N., Deka, R. & Soundalgekar, V. M.: Transient free convection flow past an infinite vertical plate with periodic temperature variation, "Journal of Heat Transfer", Vol. 4, 1091-1094 (1999).
